SEISMIC TOMOGRAPHY TO IMAGE COAL STRUCTURE STRESS DISTRIBUTION

By E. C. Westman,[1] M. J. Friedel,[2] E. M. Williams,[1] and M. J. Jackson[2]

ABSTRACT

Stress anomalies in the vicinity of the longwall face in an underground coal mine can result in violent coal bumps, compromising the safety and efficiency of mine workers. The U.S. Bureau of Mines (USBM) is using seismic tomography to monitor distribution and relative magnitude of stress concentrations throughout a coal pillar or panel. Researchers with the USBM have performed tomographic imaging in pillars and panels of Western underground longwall coal mines in support of the continuing goal of improving safety for and efficiency of underground miners.

Results of three case studies are presented. In the first case study, tomographic images of yield pillars adjacent to a mined panel were calculated. At one site, surveys were completed on subsequent days, resulting in determinations of stress redistribution as the face retreated to within 20 m (65 ft) of the pillar. In the second case study, the results of two surveys across the longwall panel as the forward abutment stress moved into the study area are described. The velocity results were compared to stress levels measured with borehole pressure cells. The final case study reports results of a survey in which a longwall shearer was used as the seismic source, rather than the hammer used in the first two studies.

INTRODUCTION

The rate of advance of longwall faces is the highest in history. With continued acceleration predicted, miners need a technique that will allow them to foresee stress-induced hazards before these hazards cause injury and downtime. Seismic tomography is being developed to create images of the interior of the coal panel in support of the U.S. Bureau of Mines (USBM) program to improve the health, safety, and efficiency of underground miners. The goal of this research is to provide the mining industry with a near real-time methodology for producing a continuously updated contour map of the stress distribution within the interior of a longwall panel and nearby pillars in the forward abutment zone. This paper describes the results of a series of seismic tomographic surveys performed at two Western longwall coal mines. The goal of these studies was to map changing stress concentrations in coal structures during longwall panel mining.

A relationship between stress and seismic wave velocity and attenuation is fundamental to these studies. Previous laboratory research (*1-2*)[3] has shown that as stress increases, alterations to the physical makeup of the material cause cavities within the material to close in the direction of primary stress, resulting in higher seismic wave velocities and lower attenuation. Under continued loading, as failure is approached, microcracks oriented parallel to the direction of primary stress form within the sample; these eventually coalesce into macrocracks just prior to failure. Opening these cracks results in lower seismic

[1]Geophysical engineer, Denver Research Center, U.S. Bureau of Mines, Denver, CO.

[2]Geophysicist, Twin Cities Research Center, U.S. Bureau of Mines, Minneapolis, MN.

[3]Italic numbers in parentheses refer to items in the list of references at the end of this paper.

wave velocities and increased attenuation. A similar response occurs during mining on a larger scale in pillars and panels.

Initiation of a seismic event, whether because of hammer impact, material failure, or some other reason, results in the generation of several different seismic wave types. These wave types have differing sensitivities to physical property changes because their modes of propagation are different. The fastest waves are compressional, or P-, waves. P-waves propagate with particle motion parallel to the direction of propagation. Slower shear, or S-, waves propagate with particle motion orthogonal to the direction of propagation. These different wave modes will also have different sensitivities to fracture orientations. Because the forward abutment stress is primarily a vertical load that closes horizontal fractures, vertically oriented shear waves are the most diagnostic of forward-abutment stress levels (*3*).

Underground tomographic surveys require the proper equipment and methodology. The USBM has developed an intrinsically safe in-seam seismic system (ISISS) to enable seismic studies in return air. The seismic data acquisition system consists of off-the-shelf components chosen because of their low cost and general accessibility. A source that delivers a high-energy signal, that is acceptable to the mine, and that is easy to use is essential. Geophones, small sensors that convert mechanical movement to electrical current, are isolated by circuit barriers housed in a steel enclosure for added durability and safety. The input and output connectors for the barrier box are NK-27 connectors, which are standard for the seismic industry. The recording instrument is a 24-channel digitizing seismograph that converts the analog voltage from the geophones into a digital representation for storage and processing. For use in the field, cables from the geophones to the barrier box are limited to four conductors, or two geophones per cable. This necessitates stringing several individual cables but provides increased safety; in case of a ground fall, there is less chance of the cable housing being compromised and several conductors shorting out.

Tomography is a method of generating images of structural features within a body by propagating energy through the body from multiple viewing angles and reconstructing pictures representative of the interior (*4*). The path followed by a seismic wave from a source to a receiver is represented as a ray (figure 1). Travel-time tomography creates a velocity distribution based on the time it takes for each ray to travel from a source to a receiver. A description of the stress level within the pillar or panel can be interpreted from the velocity tomograms. Successive tomograms taken over time as mining progresses show velocity changes in the coal as a function of changing stresses.

Originally developed for medical purposes, the method has been applied to creating cross sections of the earth using electromagnetic (*5*) and seismic waves (*6*). Recently, seismic tomography has been used to characterize stress in underground hard rock (*7-8*) and coal (*9-10*) mines.

MIGRATOM, a wave migration tomography code developed by the USBM, was used to perform tomographic reconstructions from the travel times for each survey. This code uses the simultaneous iterative reconstruction technique (SIRT) with straight rays or curved rays traced according to Huygen's principle (*11*). The root mean square residual difference between calculated and measured travel times is calculated for each iteration, showing when the solution has stabilized.

The results of three case studies are presented. In the first, the stress-induced velocity changes in the floor beneath two yield pillars were measured. The second study, at a different mine, imaged stress-induced velocity changes measured through the coal in the forward abutment of the longwall panel. The final study, conducted at the same mine as the first study, presents results of attenuation tomography studies in which the vibrations emitted by the longwall shearer were measured in the tailgate roof and analyzed for stress-induced amplitude changes.

Figure 1
Schematic of Seismic Tomography.

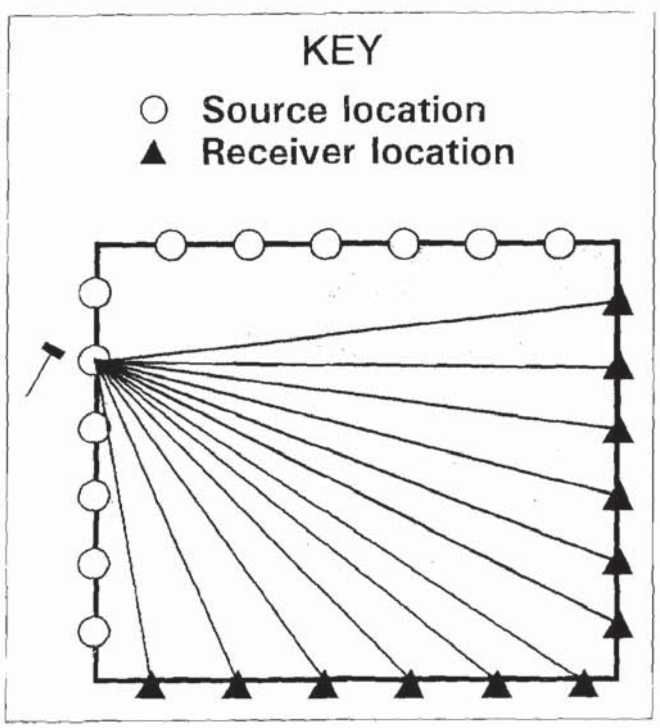

A seismic source, such as a hammer or explosive, transmits an elastic wave that is recorded by several receivers mounted on the opposite side.

CASE STUDY 1

Seismic tomography was performed through a sandstone layer in the floor beneath two yield pillars in the vicinity of the face, yet at separate locations and with different floor conditions, in a Western longwall mine (*9*). At these two underground study sites, seismic energy was excited at points on the mine floor (i.e., the underlying sandstone or mudstone) using a sledgehammer as the impact source. At site A, the propagation path of the first-arrival wave involved travel from the point of impact, across a sandstone member, to the geophones placed in the mine floor. At site B, the refracted wavelet traveled from the point of impact, through a mudstone layer, along the top of the sandstone, and back through the mudstone to the geophones placed on the mine floor (figure 2).

DATA ANALYSIS

Seismic tomography may require making static corrections to the original data. Static corrections are necessary to remove time delays associated with travel through "slow" strata, i.e., strata in which the seismic wave travels significantly less quickly than in the primary strata being observed. Because the objective of this study was to generate images of velocity distributions in the sandstone, it was important to remove time delays associated with travel through the mudstone. To achieve this goal, first-arrival travel-time measurements were plotted as a function of source-receiver separation for each side of the pillar. Because the actual propagation path was not known, the distance between any given source-receiver pair was assumed to be straight. Despite the scattering of data (attributed to the assumption of straight ray paths instead of the probable curved ray paths and local variations in both loading and random noise), linear trends are evident in the time-distance plots shown in figure 3.

VELOCITY DISTRIBUTION: SITE A

Figure 4 shows the velocity tomogram for study site A when the center of the pillar and longwall face were separated by a distance of about 30 m (100 ft). The characteristic velocity structure was heterogeneous, having several seemingly random but localized high-velocity regions [4 km/s (13,000 ft/s)] overprinted on a uniform background velocity [2 km/s (6,500 ft/s)]. The consistent and pervasive nature of these velocity features, despite the use of various starting velocity models and constraints, suggested that they were probably stress related and not artifacts of the tomographic program. While it is tempting to assign a value of stress to the computed velocities, it must be recalled that the accuracy of reconstructed velocity extremes is sensitive to the degree of sampling (number of ray paths) and so are most accurate as indicators of stress distribution, not necessarily absolute stress magnitude.

Figure 5 shows a velocity tomogram generated after a day of mining at site A. In this case, the longwall face had retreated to within 18 m (60 ft) of the center of the pillar. Again, the velocity distribution was heterogeneous, ranging from 2 to 4 km/s (6,500 to 13,000 ft/s); however, the high-velocity regions shifted toward the center of the pillar and intensified. Also notable was the development near the pillar core of a high-velocity region trending perpendicular to the direction of primary cleating.

The change in velocity character at site A from one tomogram to the next implied that temporal variations in stress occurred. To better define those regions of greatest change in mechanical conditions, a difference tomogram was computed (figure 6) by subtracting the first reconstruction from the second. This tomogram indicated that the greatest stress increase occurred along entry 2 from the center of the pillar to the outby end of the pillar, and also in the outby corner of the pillar nearest to the panel. At the center of the pillar, only a minor increase in stress [as indicated by a 0.5-km/s (1,640-ft/s) velocity increase] was observed.

VELOCITY DISTRIBUTION: SITE B

Figure 7 shows the velocity distribution for site B at a time when the longwall face was roughly 18 m (60 ft) inby the center of the pillar. Again, the velocity structure appeared heterogeneous [spanning 2 to 4 km/s (6,500 to 13,000 ft/s)], suggesting that stress was being applied nonuniformly to the pillar. The velocity systematically decreased along the center axis (parallel to the panel) of the pillar and away from the working face. The region of greatest concentrated stress appeared at the pillar end closest to the longwall face, manifesting itself as a region of concentrated stress both directly under and extending away from the pillar. Furthermore, the buildup of stress along a direction perpendicular to the primary cleat was similar to that observed during the second survey at site A; however, in this case, the buildup appeared to have shifted toward the center of the pillar.

CASE STUDY 2

Two seismic surveys were performed across a 215-m (700-ft) wide coal panel in an underground mine in an effort to generate images of the onset of the forward abutment stresses (*12*). Source and receiver locations were spaced at 6-m (20-ft) intervals on opposite sides of the panel. Typically, the forward abutment stress retreats with the face, staying within approximately 30 m (100 ft) of the face. Two surveys were completed, one when the working face was 25 m (80 ft) from the survey area, and the second after the face had retreated to within 8 m (25 ft) of the survey area (figure 8). The 40-Hz, three-component geophones were firmly anchored in 1-m (3-ft) boreholes along the headgate entry 3 panel rib.

The source was a sledgehammer struck against the panel rib at points spaced every 6 m (20 ft) along tailgate entry 1. The occasional presence of soft coal along the panel entry required the use of a steel rod with the hammer to couple the energy to the unfractured coal within the panel. The hammer was swung up to 30 times per location, and for each impact, the data were converted to digital memory. Each record was stacked with the previous ones to increase the signal strength relative to the background noise. It was discovered after the first survey that there was a high amount of microseismic activity that would occasionally mask the signal of the transmitted wave. During the second survey, the stack preview capability of the seismograph was used to delete any records in which significant microseismic noise was present. Records free of microseismic noise were stacked by the seismograph, and the summed record was saved to disk.

PANEL VELOCITY DISTRIBUTIONS

A distinct change in stress distribution at the working face of the panel is illustrated by comparing the velocity tomograms for the two surveys. Velocities of the vertically oriented shear (SV) waves were used because they are the most sensitive to the effects of vertical stresses (*3*). The SV velocity distribution for the first survey (figure 9) is quite uniform, having a mean velocity of 0.89 km/s (2,940 ft/s), with a standard deviation of 0.07 km/s (230 ft/s.) The SV velocity distribution for the survey taken the second day has a mean velocity of 0.89 km/s (2,920 ft/s), with a standard deviation of 0.06 km/s (200 ft/s); however, figure 10 shows two clear velocity peaks within the panel, one near the intersection of the face and the tailgate, and the other 35 m (115 ft) outby the face along the headgate. The peaks result from movement of the forward abutment stresses into the survey area. The stress on the coal panel is greatest in the vicinity of the least support, where the tailgate intersects the working face, resulting in the highest velocity measurements. The second velocity peak shown in the figure occurs outby the face, along the headgate; a low-velocity zone exists at the intersection of the face and headgate. One possible explanation is that the stress in this area bridges over to the adjacent unmined panel, thereby destressing the face. Additionally, the primary cleat direction trends northeast-southwest at this mine, possibly resulting in increased fracturing and a lowered velocity region at the junction of the face and the headgate.

COMPARISON OF PANEL VELOCITIES WITH BOREHOLE PRESSURE CELL MEASUREMENTS

The SV velocity distribution from the second day was compared to measurements obtained with conventional geotechnical instruments at a point near the tailgate side of the panel. Borehole pressure cells were emplaced in the panel to monitor stress changes at a single point during mining. Borehole pressure cells are flat steel bladders, approximately 5 cm wide by 20 cm long (2 in by 8 in), filled with hydraulic oil. The cell is grouted several meters into a borehole, and an initial pressure is established in the cell closely approximating the anticipated load on the cell. A tube connects the cell to a pressure transducer outside the coal. As pressure within the coal increases, the cell is deformed. The pressure transducer converts the subsequent change in oil pressure to a change in electrical voltage, which is recorded on a data logger (*13*). The velocity distribution for a profile located 12 m (40 ft) into the coal from the east side of the panel can be compared to stress change measurements obtained at different times as the face approaches the location of a from a single borehole pressure cell installed 12 m (40 ft) the panel rib (figure 11). The six velocity points displayed are the calculated values within the tomogram along the profile. The figure shows that the SV results correlate well to the stress measurements.

CASE STUDY 3

Studies were performed on a Western longwall panel (at the same mine as case study 1) in an initial effort to determine if a longwall shearer could be used to obtain images of stress distribution in the immediate vicinity of the face and tailgate. Use of the shearer would allow safer and more automated data acquisition, as well as enable the generation of images of the immediate face area of the panel. The amplitude of the grinding action of the longwall shearer was assumed to be approximately constant relative to amplitude changes caused by stress-induced physical property changes within and adjacent to the coal seam. By calculating the amplitude at specific points, tomographic images of attenuation in the longwall panel were obtained.

Surveys were conducted by recording the signals from geophones in the tailgate when the shearer was at specific locations along the face. A display of shearer position on the headgate shield allowed an observer at the headgate to trigger the seismograph manually as the shearer passed every fifth shield, approximately every 7 m (23 ft). Geophones were attached to roof bolts in the tailgate at approximately 15-m (50-ft) intervals. Attaching the geophones to roof bolts was much easier than drilling boreholes into the rib; however, this method resulted in a survey of the immediate roof rather than the coal seam. Receivers could not be attached to roof bolts in the headgate because vibrations from the conveyor belt would mask any signal from the shearer.

Processing the data consisted of calculating the amplitudes and generating the attenuation tomograms. The amplitudes used as input to the tomography program were calculated by obtaining the average periodogram for the recorded signal between 80 and 200 Hz (*14*). These amplitudes were then converted to the appropriate units for input to MIGRATOM (*11*). The calculation required a value for the input amplitude; because no sensor could be placed in the immediate vicinity of the longwall shearer as it moved across the face, the received amplitudes were plotted as a function of distance, and an estimate of the

Figure 2
Refracted Ray Path Beneath Coal Pillar (Not To Scale).

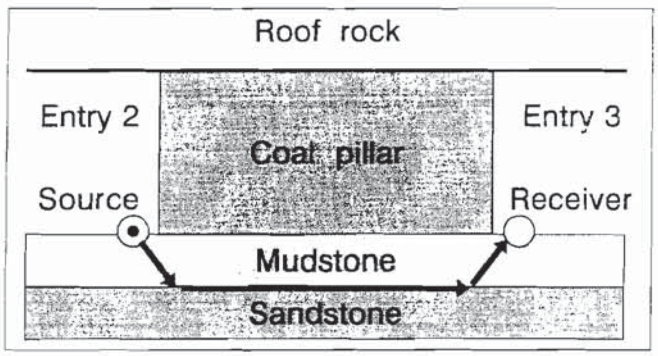

Figure 3
Travel-Time Scatterplots.

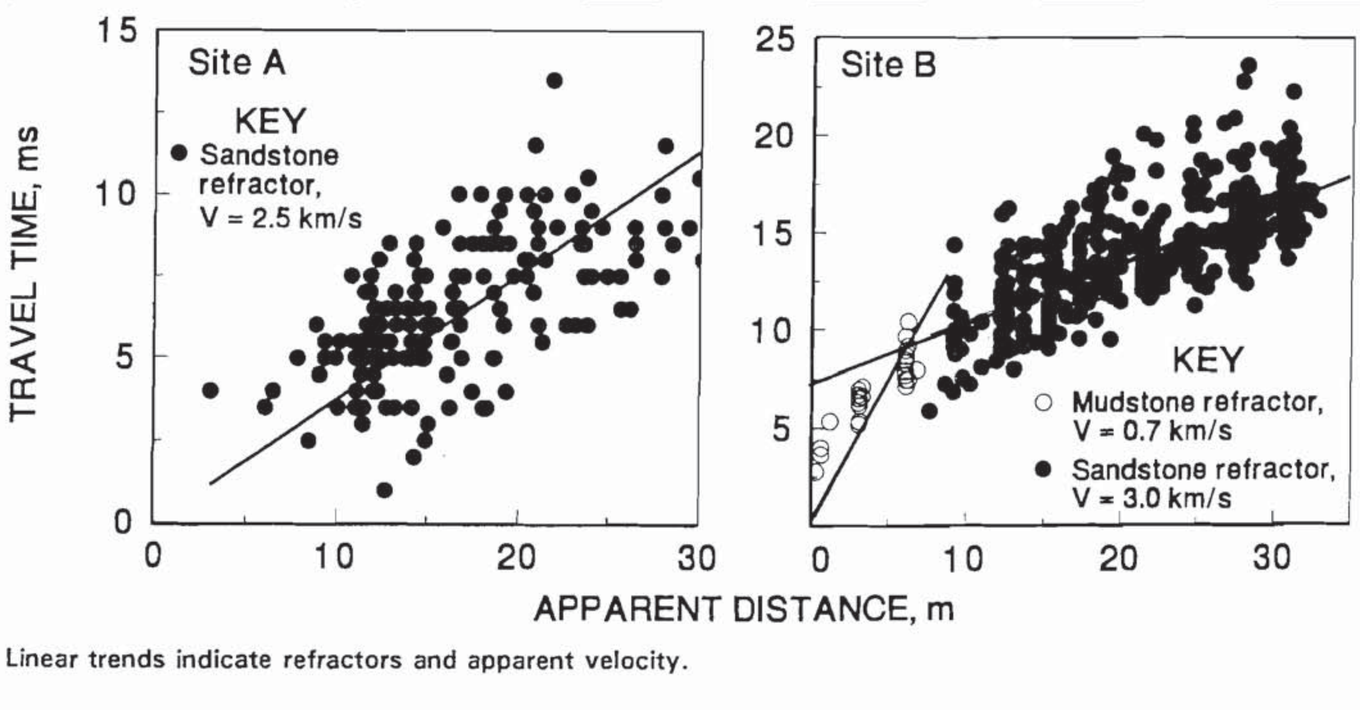

Linear trends indicate refractors and apparent velocity.

input amplitude was obtained by extrapolating back to zero offset.

A triangular image was obtained from the tomographic reconstruction because the receivers were only placed in the tailgate. Limitations in the angle of coverage restricted interpretation of the image to regions approximately 60 m (200 ft) wide along the face and the tailgate. The region along the tailgate was examined for this study, resulting in a rectangular plot 60 m (200 ft) wide by 100 m (330 ft) long.

Figure 12 shows the attenuation tomograms calculated for 2 days as the face retreated. The images are similar between 370 and 430 m east and show several features ahead of the face that were constant from one day to the next, presumably due to geologic anomalies in the roof. Typically, high attenuation identifies a material with open cracks (due either to low stress or failed material); therefore, the high attenuation region at the junction of the face and the tailgate, extending approximately 25 m (80 ft) along the tailgate for both days, indicates a material with open cracks. As this is the location of expected high stress, two explanations are possible: (1) the roof through which these surveys were taken is cantilevering over the gob, opening cracks within it or (2) the stress within the roof is approaching failure stress, and fractures are being created prior to failure. Without additional information it is not possible to determine precisely what is occurring in the roof; however, future studies will allow further development of this potentially useful technology.

Figure 4
P-Wave Tomogram, Site A, Day 1.

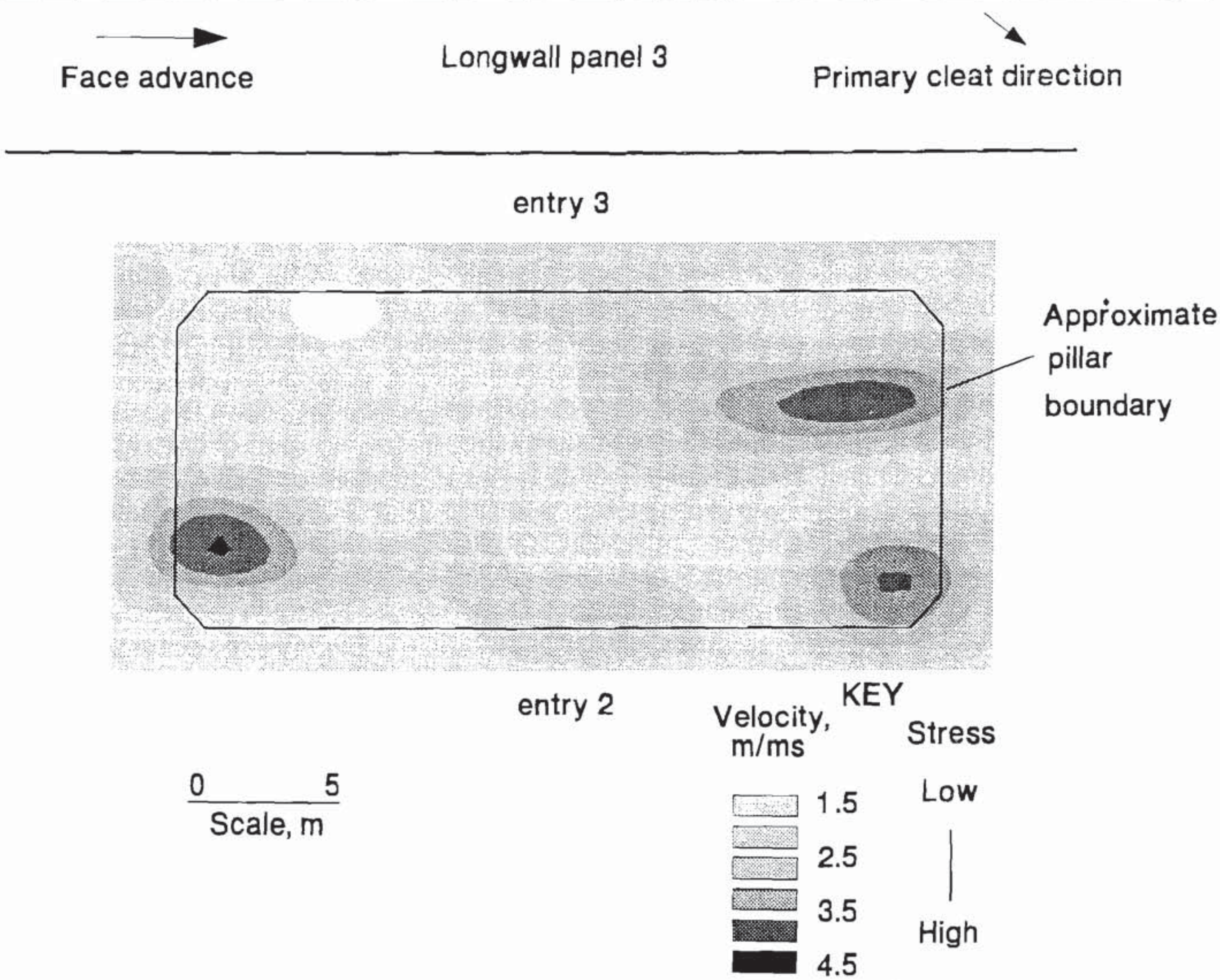

Pillar center is 22 m (72 ft) from face. High-velocity regions indicate concentrated loading.

Figure 5
P-Wave Tomogram, Site A, Day 2.

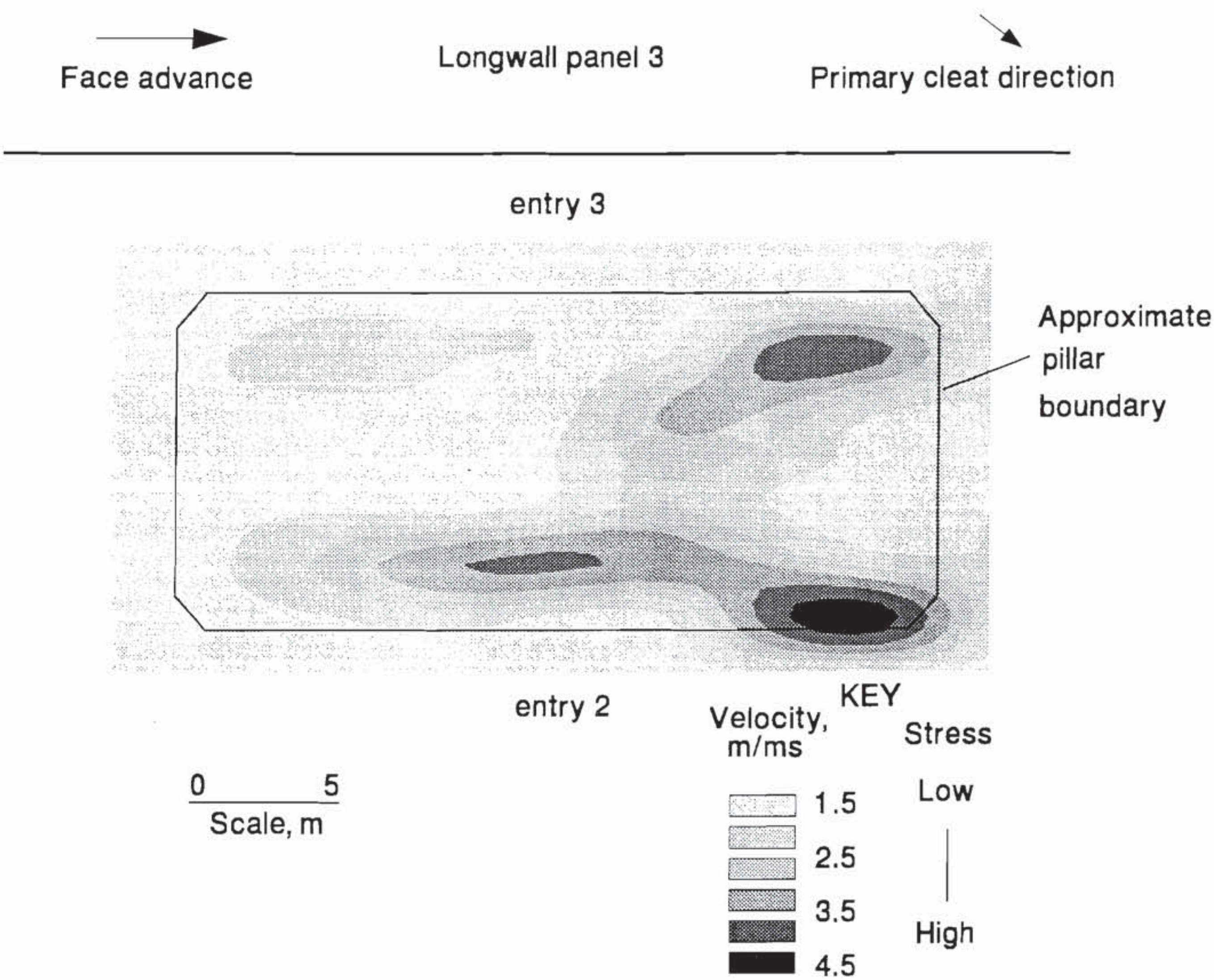

Pillar center is 9.5 m (30 ft) from face. High-velocity regions indicate stress buildup along a trend perpendicular to primary cleat.

Figure 6
P-Wave Difference Tomogram, Site A.

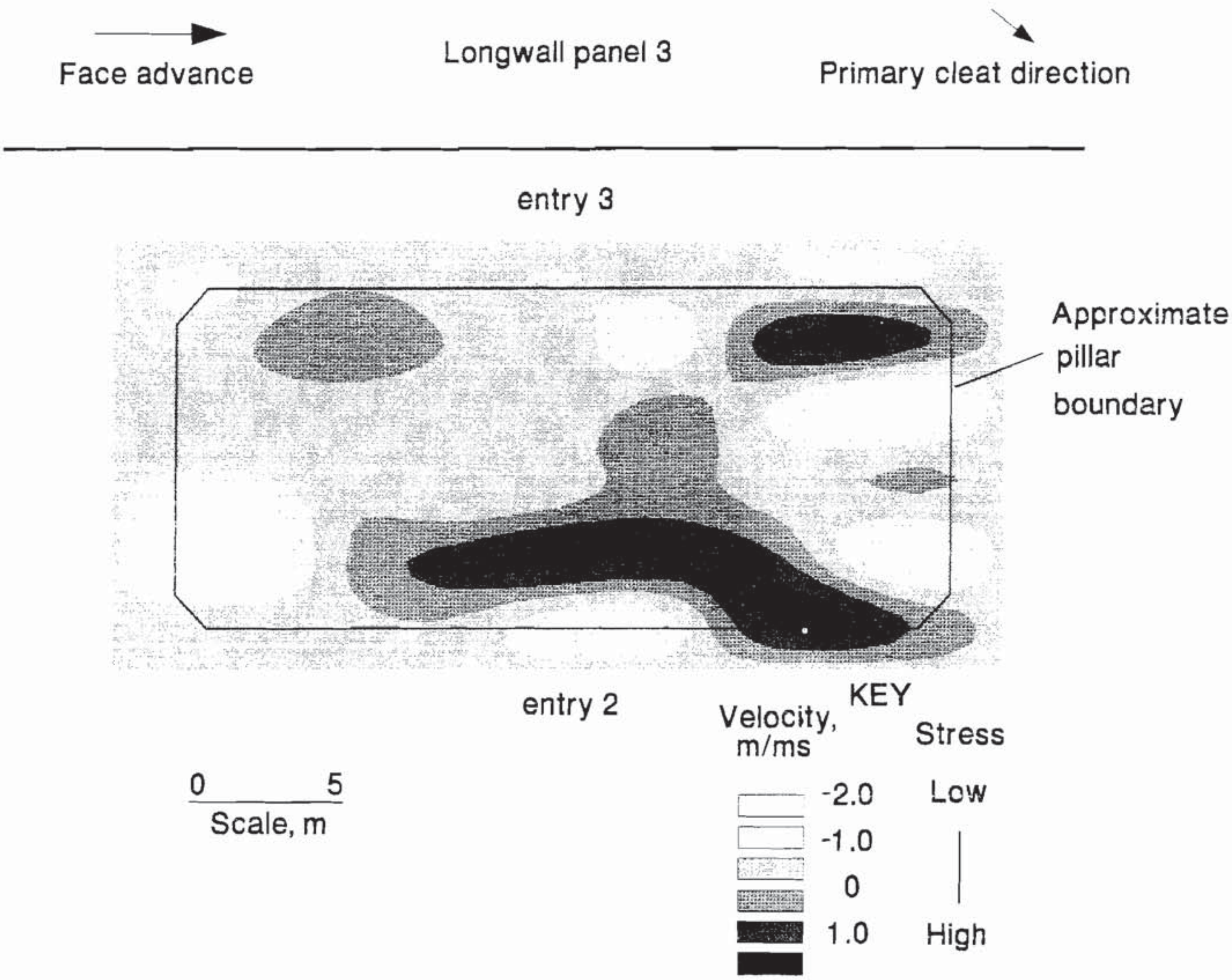

Tomogram indicates buildup (velocity increase) and relaxation (velocity decrease) of mine structure.

Figure 7
P-Wave Tomogram, Site B.

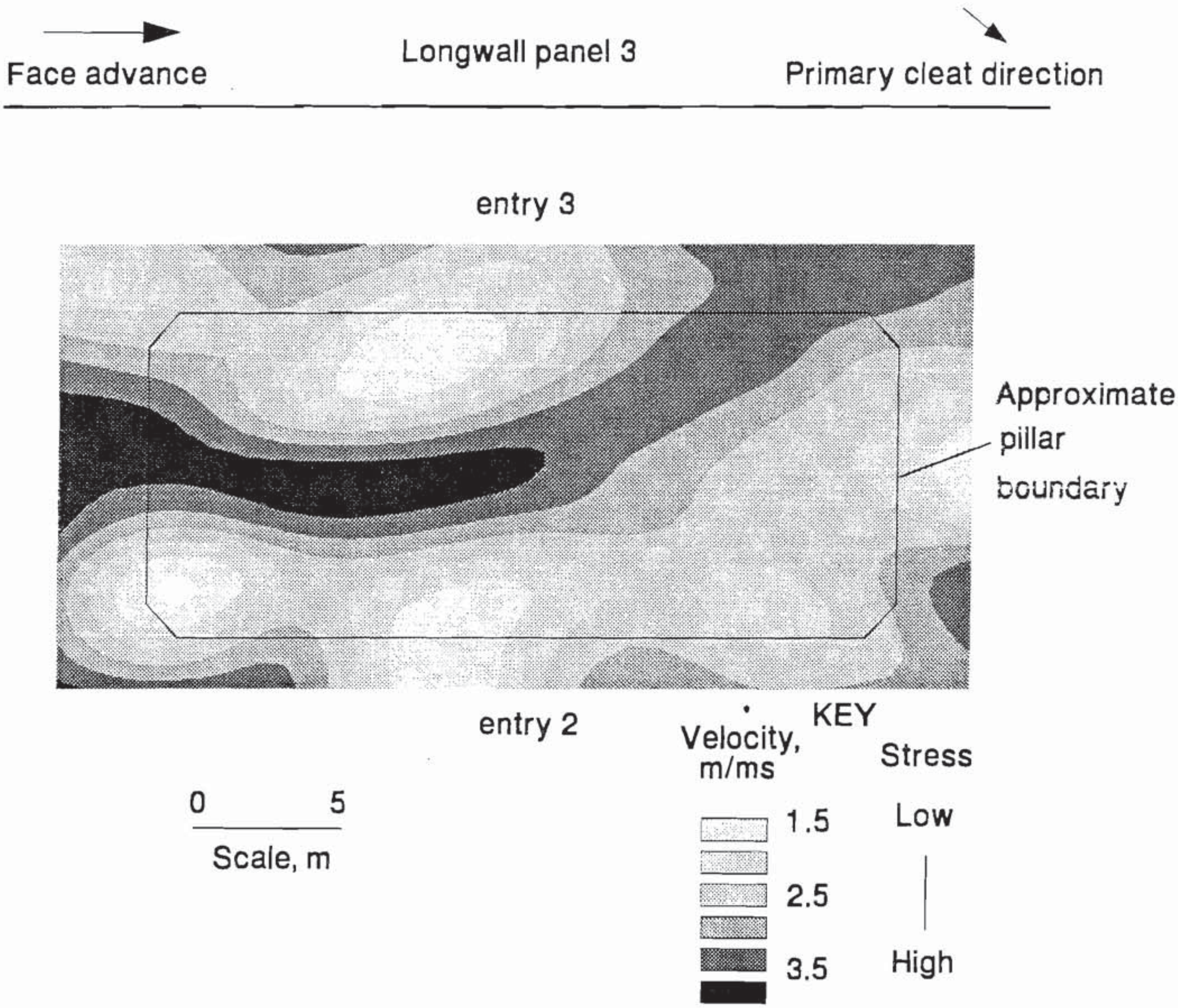

Tomogram indicates stress buildup at pillar end closest to working face and along trend perpendicular to primary cleat.

Figure 8
Map of Survey Area for Panel Study.

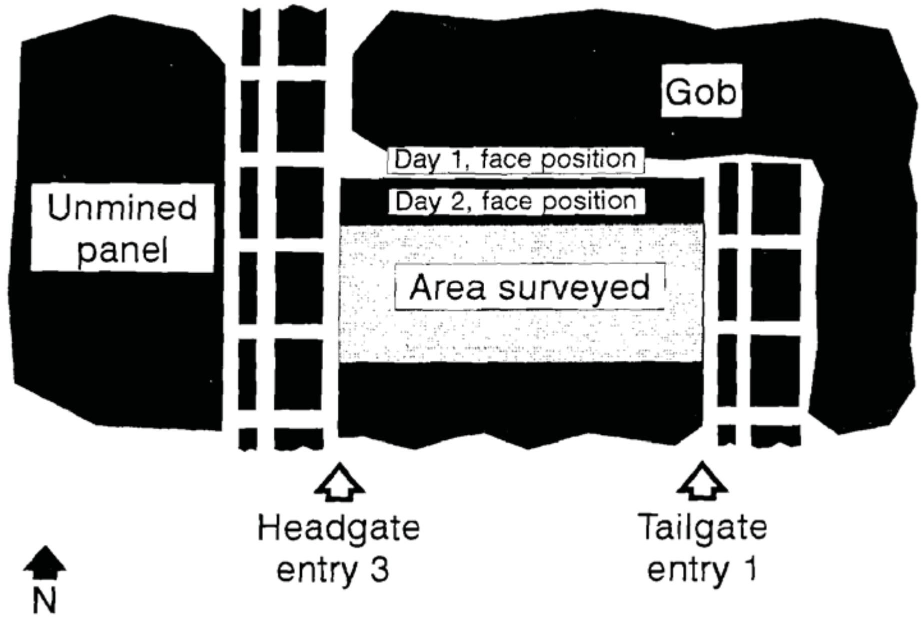

Face locations are indicated for the two study periods.

Figure 9
SV Velocity Tomogram for Survey Taken on Day 1.

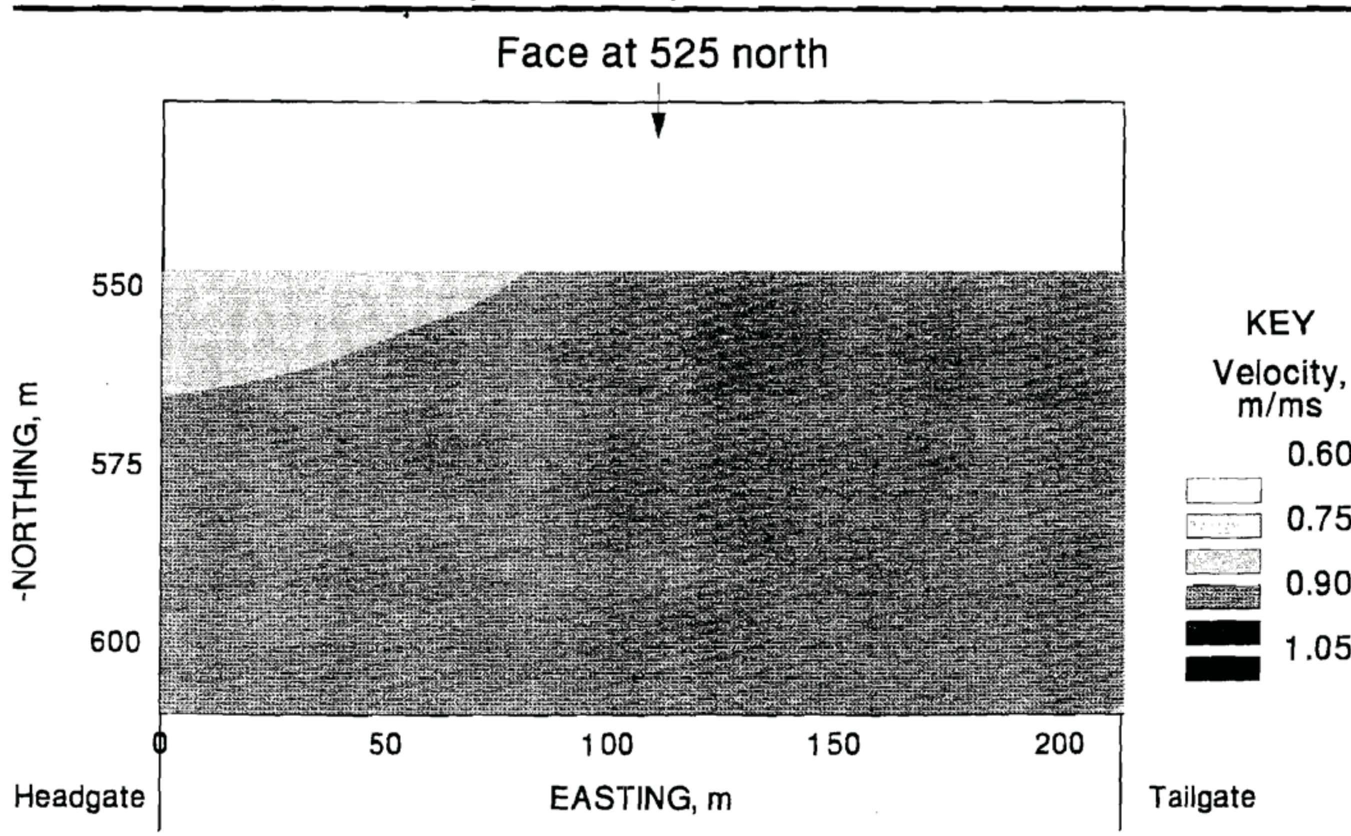

Working face is 24 m (80 ft) north of survey area.

Figure 10
SV Velocity Tomogram for Survey Taken on Day 2

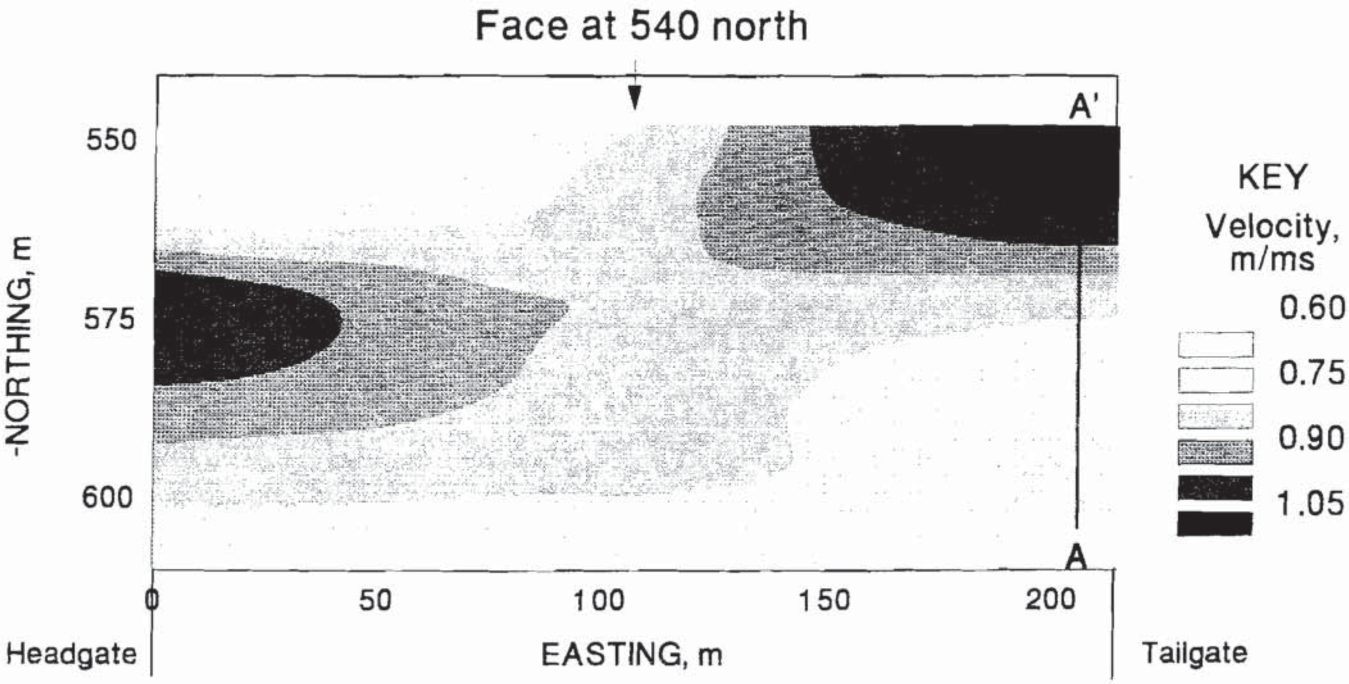

Working face is 8 m (25 ft) north of survey area. Profile A-A' is shown parallel to east edge of panel.

Figure 11
Comparison of Calculated Velocity Profile A-A' (See Figure 10) With Data From BPC.

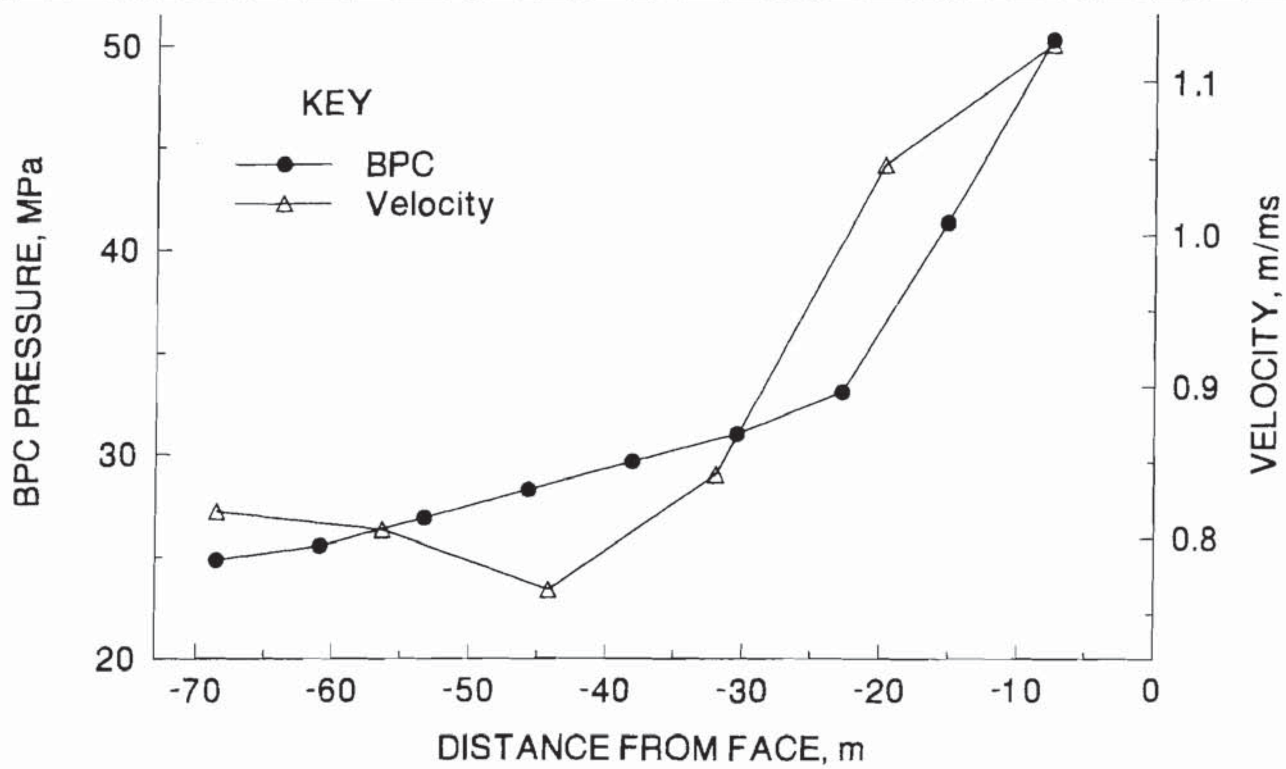

BPC was installed 12 m (40 ft) into panel. Pressure values were collected from different face positions.

Figure 12
Attenuation Tomograms of Panel Within 60 m (200 ft) of Tailgate.

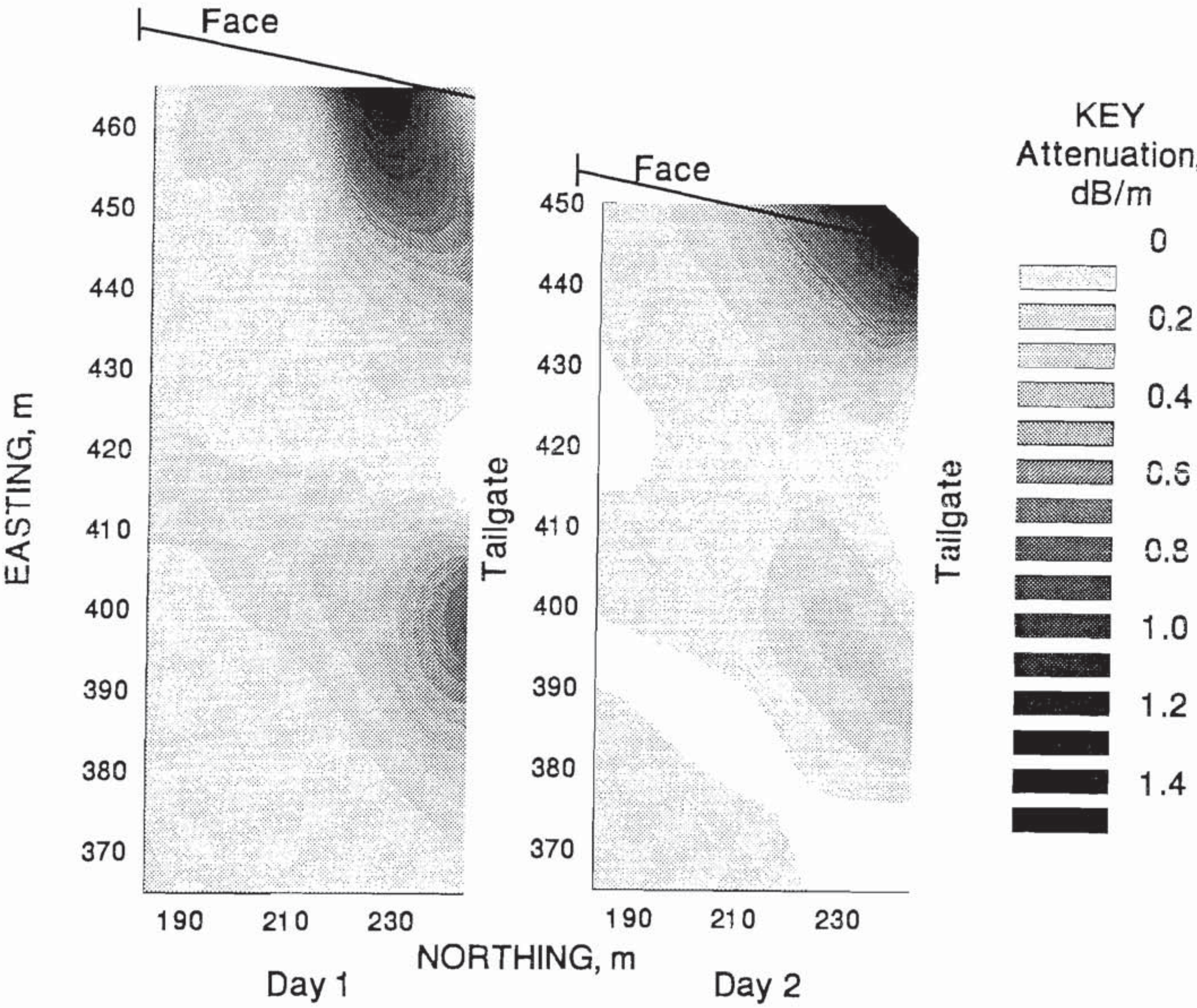

High-attenuation regions near face indicate concentrated loading of forward abutment.

CONCLUSIONS

Seismic tomographic surveys were performed in three case studies. In the first case study, velocity distributions were determined in the floor beneath yield pillars in the headgate near the longwall face. A high-velocity core, which is indicative of high stress, perpendicular to the primary cleat was observed. With the exception of localized failure zones, P-wave velocity increased as the face retreated to within 18 m (60 ft) of the center of the pillar on a subsequent survey, indicating a general stress buildup within the pillar as the face approached.

The second case study mapped the longwall panel as the forward abutment stress moved into the region. An area 60 m (200 ft) long by the entire width of the panel [210 m (700 ft)] was mapped on successive days as the face retreated to within 8 m (25 ft) of the survey area. A region of high shear-wave velocity was observed near the junction of the face and the tailgate. A cross section of the velocity image correlated well with stress measurements obtained from borehole pressure cells.

The final case study detailed an effort to map the panel within 60 m (200 ft) of the tailgate ahead of the face by using the longwall shearer as the seismic source. By assuming a relatively constant level of noise produced by the shearer, attenuation tomograms were generated that allowed inference of geologic and stress anomalies near the junction of the face and the tailgate.

Seismic tomography offers a unique tool to the mining industry. Combining the methods described in this paper with automated acquisition could allow a mine engineer to have continuous updating of the distribution of stress concentrations and geologic anomalies in underground structures. These factors can be examined, and in the case of hazardous conditions, appropriate actions can be taken prior to compromising safe working conditions.

REFERENCES

1. Yu, G. Elastic Properties of Coals. Ph. D. Thesis, MacQuarie Univ., Sydney, Aust., 1992, 133 pp.

2. Shea-Albin, V. R., D. R. Hanson, and R. E. Gerlick. Elastic Wave Velocity and Attenuation as Used To Define Phases of Loading and Failure in Coal. USBM RI 9355, 1991, 43 pp.

3. Westman, E. C., M. M. Foss, and E. M. Williams. Comparison of Stress Distribution Images Generated with P, SH, and SV Velocity Tomograms. Paper in Expanded Abstracts of the 64th Society of Exploration Geophysicists Annual Meeting (Los Angeles, CA, Oct. 23-28, 1994). Soc. Expl. Geophys., 1994, pp. 544-546.

4. Gordon, R. A Tutorial on ART (Algebraic Reconstruction Techniques). IEEE Trans. Nucl. Sci., v. NS-21, June 1974, pp. 78-93.

5. Dines, K. A., and J. R. Lytle. Computerized Geophysical Tomography. Proc., IEEE, v. 67, No. 7, July 1979, pp. 1065-1073.

6. Mason, I. M. Algebraic Reconstruction of a Two-Dimensional Velocity Inhomogeneity in the High Hazles Seam of Thoresby Colliery. Geophys., v. 46, 1981, pp. 298-308.

7. Young, R. P., and S. C. Maxwell. Seismic Characterization of Highly Stressed Rock Mass Using Tomographic Imaging and Induced Seismicity. J. Geophys. Res., v. 97-B9, 1992, pp. 12361-12373.

8. Maleki, H. The Application of Tomographic Methods for the Study of Structural Failure. Paper in Proceedings: Mechanics and Mitigation of Violent Failure in Coal and Hard-Rock Mines. USBM Spec. Publ. 01-95, 1995, pp. 313 to 322.

9. Friedel, M. J., M. J. Jackson, E. M.Williams, and M. S. Olson. Tomographic Imaging of Coal Pillar Conditions: Observations and Implications. Soc. Min. Eng. preprint 94-265, 1994, 19 pp.

10. Westman, E. C. Characterization of Structural Integrity and Stress State via Seismic Methods: A Case Study. Paper in Proceedings of 12th International Conference on Ground Control in Mining, ed. by S. S. Peng (Morgantown, WV, Aug. 3-5, 1994). Dep. of Min. Eng., WV Univ., 1993, pp. 322-329.

11. Jackson, M. J., and D. R. Tweeton. MIGRATOM - Geophysical Tomography Using Wavefront Migration and Fuzzy Constraints. USBM RI 9497, 1994, 35 pp.

12. Williams, E. M., and E. C. Westman. Stability and Stress Evaluation in Mines Using In-Seam Seismic Methods. Paper in Proceedings of 13th International Conference on Ground Control in Mining, ed. by S. S. Peng (Morgantown, WV, Aug. 2-4, 1994). Dep. of Min. Eng., WV Univ., 1994, pp. 290-297.

13. Haramy, K. Y., and R. O. Kneisley. Hydraulic Borehole Pressure Cells: Equipment, Technique, and Theories. USBM IC 9294, 1991. 26 pp.

14. Stearns, S. D., and R. A. David. Signal Processing Algorithms in Fortran and C. Prentice-Hall, 1993, 331 pp.

Special Publication 01-95

Proceedings: Mechanics and Mitigation of Violent Failure in Coal and Hard-Rock Mines

Edited by Hamid Maleki, Priscilla F. Wopat, Richard C. Repsher,
and Robert J. Tuchman

UNITED STATES DEPARTMENT OF THE INTERIOR
Bruce Babbitt, Secretary

BUREAU OF MINES
Rhea L. Graham, Director

Library of Congress Cataloging in Publication Data:

Maleki, Hamid N.

Proceedings : mechanics and mitigation of violet failure in coal and hard-rock mines / edited by Hamid Maleki ... [et al.].

p. cm. — (USBM special publication; 01-95)

Includes bibliographical references.

Supt. of Docs. no.:I 29.151 : 01-95.

1. Rock bursts—Congresses. 2. Mine roof control—Congresses. 3. Coal mines and mining—Safety measures—Congresses. 4. Mines and mineral resources—Safety measures—Congresses. I. Title. II. Series: Special publication (United States. Bureau of Mines); SP 01-95.

TN317.M35 1995 622'.28—dc20 95-7138 CIP